Global Advanced Research Journal of Physical and Applied Sciences Vol. 4 (1) pp. 064-071, September, 2015
Available online http://www.garj.org/garjpas/index.htm

Full Length Research Paper

Subsurface Resistivity Structures of Some Parts of Southern Upland Area of River Kaduna, North Central Nigeria

Alkali SC

Department of Geology, University of Maiduguri, P. M. B. 1069, Maiduguri, Nigeria
Email: samcrah@gmail.com, Tel: +2348069263114

Accepted 29 September, 2015

Shallow subsurface electrical resistivity images of Southern Upland area of River Kaduna defined fresh geoelectric basement at different levels. While some parts of the bedrock topography outcropped on the surface, others are buried beneath weathered sediments. Fracturing probably split and displaced the bedrocks into individual granite blocks along weak zones. The blocks that resisted weathering stood as isolated hill summits. Where the bedrock nears the surface, effect of fracturing is low. Development of deep fractures is however, pronounced along weak zones. At some locations the fractures extended to the surface and in others, they assumed the structural shapes initiated by the fresh basement. Formation of ridge structures and characteristic dome-tops is probably due to resistance of the fresh bedrocks to conditions they were subjected to. The main weathered products of the profiles are gravels with some gravelly sands, sands and clays. Some of these sediments are exposed on the surface and constitute the main capping units. At some locations they occupy existing structures of the underlying fractures and inclined diagonally along their directions. Depression of underlying rock units housed considerable quantity of arenaceous sediments around some localities. Thickness of weathered regolith within two major fractured zones exceeded 30 m. Minimum thickness of the overburden is estimated at 7 m. Within the highly fractured zones clay matrix constitute minor constituents of the overburden. Clay sands occurred in patches and are enveloped by thin layers of sandy fractions in some locations.

Keywords: Dipole-dipole, resistivity, profile, bedrock, structures, fractures,

INTRODUCTION

Geophysical resistivity techniques are based on the response of the earth to the flow of electrical current. In these methods, an electrical current is passed into the ground through two current electrodes and two potential electrodes record the resultant potential difference between them, and thereby providing a way of measuring the electrical impedance of the subsurface material. The apparent resistivity is then a function of the measured impedance and the geometry of the electrode array. Depending upon the survey geometry, the apparent resistivity data may be plotted as 1-D soundings, 1-D profiles, or 2-D cross-sections.

In the shallow subsurface, the presence of water controls much of the conductivity variation. Measurement of resistivity is, in general, a measure of water saturation and connectivity of pore space. Increasing saturation, increasing salinity of the underground water, increasing porosity of rock and increasing number of fractures all tend to decrease measured resistivity (Loke, 2004). Increasing compaction of soils or rock units will expel water and effectively increase resistivity. Air, with naturally high resistivity, results in the opposite response compared to water when filling voids. Whereas the presence of water will reduce resistivity, the presence of air in voids should increase subsurface resistivity.

Resistivity measurements are associated with varying depths of investigation depending on the separation of the current and potential electrodes in the survey, and can be interpreted in terms of a lithologic and/or geohydrologic model of the subsurface (Telford et al, 1976; Kearey and Brooks, 1991; Burger, 1992).

The use of dipole-dipole array in electrical prospecting has become common. In terms of logistics on the field, it is the most convenient especially for large spacing. This is because other arrays require significant lengths of wire to connect the power supply and voltmeter to their respective electrodes and the wire must be moved for every change in spacing as the array is either expanded for a sounding or moved along a line. The convention for dipole-dipole array is that current and potential electrode spacing is the same, **a**, and the spacing between them is an integral multiple of **a, na**.

Kaduna city shown in Figure 1 is the capital of Kaduna State in North Central Nigeria. It is located between latitudes 10°24'N – 10°40'N and between longitudes 7°18'E – 7°42'E. The resistivity imaging is aimed at producing 2-D resistivity structures of shallow subsurface rock units using dipole-dipole electrode array.

General Geology

The Nigerian Basement complex lies east of the West African Craton and northwest of the Congo Craton in a mobile belt affected by the Pan African Orogeny. The basement rocks outcropped largely in the southwestern and north central parts of Nigeria and minimally in the northeastern and southeastern parts of the country. Rahaman (1976, 1988) classified the rocks into migmatite – gneiss – quartzite complexes: a heterogeneous group consisting of migmatitic and granitic gneisses, minor amounts of basic rocks (basic schists and amphibolites) and relict metasediments (calc-gneisses and quartzites) and the slightly migmatised to non-migmatised metasedimentary and metaigneous rocks. Rocks of this group constitute the schist belts of Nigeria and generally define the structural grain of the country. Lithologically, they are composed of pelitic to semi-pelitic schists, quartzites, polymitic metaconglomerates, calc-gneisses, marble and metaigneous rocks (amphibolites and talc-bearing actinonite-chlorite-chlorite schist).

Members of the Older Granites suite rocks are widely distributed throughout the Nigeria Basement complex and they constitute distinct plutons often of batholitic proportions. Compositionally they range from diorite to tonalite to syenite and in texture from aplite to coarse porphyritic granite.

Metamorphosed to un-metamorphosed calc-alkaline volcanics and hypabassal rocks which are restricted to the Anka Schist belt of northwestern Nigeria comprise tuffs, rhyolites, rhyodacites, and dacites. Unmetamorphosed dolerite and syenite dykes are minor rock types found as dykes emplaced in older rocks.

The study area forms part of the northwestern basement terrain underlain by basement rocks of Precambrian age. They rocks are mainly granites, gneisses, and schists. Oyawoye (1964) showed the existence of a structural relationship between the Nigerian Basement complex and the rest of the West African basement. This is partly due to the fact that the whole region was involved in a single set of orogenic episode - the Pan African orogeny, which left an imprint of similar structures upon the rock units. The gneisses are found as small belts within the granite intrusions, and are also found east and west of the batholiths. The biotite gneiss extends westwards to form a gradational boundary with the schist belt. The gneiss continues eastwards to some extent and is occasionally broken up by the Older Granite (Wright and McCurry, 1970).

The structural and tectonic framework of the Nigerian Basement complex has been reported as comprising NE - SW and NW - SE lineaments superposed over a dominant N – S trend (Olasehinde et al., 1990), and NW – SE and NE – SW pair superimposed on a N - S joint set (Annor and Freeth, 1985; Annor et al., 1990). Olasehinde et al. (1990) confirmed Ball's (1980) presence of NW – SE aeromagnetic signature which coincides with the regional patterns recorded on the basement.

MATERIALS AND METHODS

Resistivity imaging technique was developed to image the subsurface having moderately complex geology and wide variations in aquifer occurrences. It combines resistivity sounding and profiling, incorporates the effects of lateral variations in resistivity on sounding, and produces a two - dimensional subsurface resistivity image.

The dipole-dipole electrode array consists of two sets of electrodes, the current (source) and potential (receiver) electrodes (Figure 2). A dipole is a paired electrode set with the electrodes located relatively close to one another. The convention for a dipole-dipole electrode array is to maintain an equal distance for both the current and the potential electrodes (spacing = **a**), with the distance between the current and potential electrodes as an integer multiple of **a** (Loke, 1999).

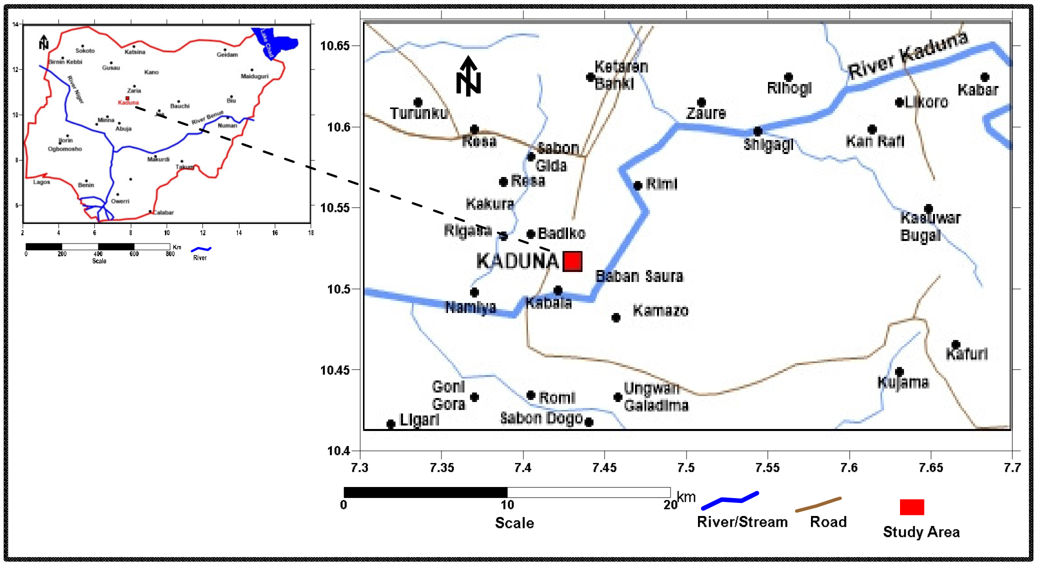

Figure 1 Location Map of the Study Area

$$\rho_A = \frac{V}{I}\pi\, a\, n(n+1)(n+2).$$

Figure 2 Dipole-Dipole configuration and apparent resistivity

For the dipole-dipole array, the measurement started with a spacing of "**1a**" between the C1-C2 (and also the P1-P2) electrodes. The first sequence of measurements was made with a value of 1 for the "**n**" factor (which is the ratio of the distance between the C1-P1 electrodes to the C1-C2 dipole length), followed by "**n**" equals to 2 while keeping the C1-C2 dipole pair spacing fixed at "**1a**". When "**n**" equals to 2, the distance of the C1 electrode from the P1 electrode was twice the C1-C2 dipole length. For subsequent measurements, the "**n**" spacing factor was increased to a maximum value of about 6 in order to increase the depth of investigation.

To plot the data from a 2-D imaging survey, the pseudosection contouring method was used. In this case, the horizontal location of the point was placed at the mid-point of the set of electrodes used to make the measurement. The vertical location of the plotting point was placed at a distance that was proportional to the separation between the electrodes.

The pseudosection plot obtained by contouring the apparent resistivity values gives a fair approximate picture of the true subsurface resistivity distribution. Figure 3 shows the resistivity pseudosections and structure of Profile 6.

Resistivity Models

Geophysical inversion seeks to find a model that gives a response that is similar to the actual measured values. The model is an idealized mathematical representation of a section of the earth. The model has a set of model parameters that are the physical quantities to be estimated from the observed data. The model response is the synthetic data that can be calculated from the mathematical relationships defining the model for a given set of model parameters. All inversion methods try to determine a model for the subsurface whose response agrees with the measured data subject to certain restrictions. The model parameters are the resistivity values while the data is the measured apparent resistivity values. The mathematical link between the model parameters and the model response for the 2-D resistivity models is provided by the finite-difference (Dey and

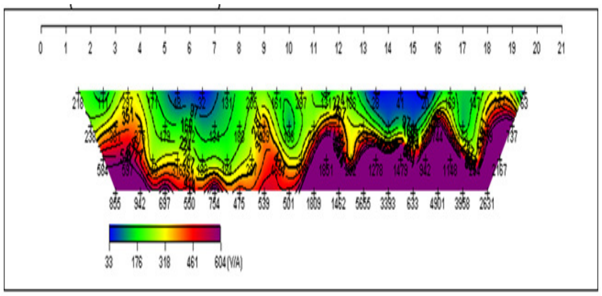

(a) Field data pseudosection

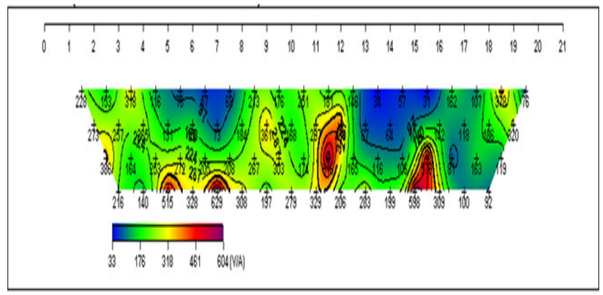

(b) Theoretical data pseudosection

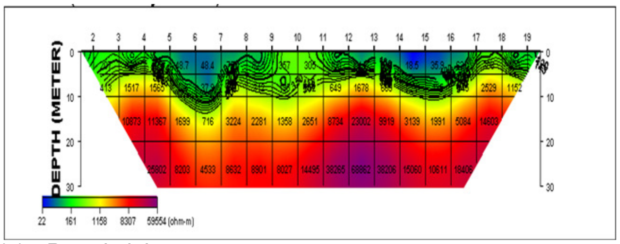

(c) 2D resistivity structure

Figure 3 Resistivity Images of Profile 6

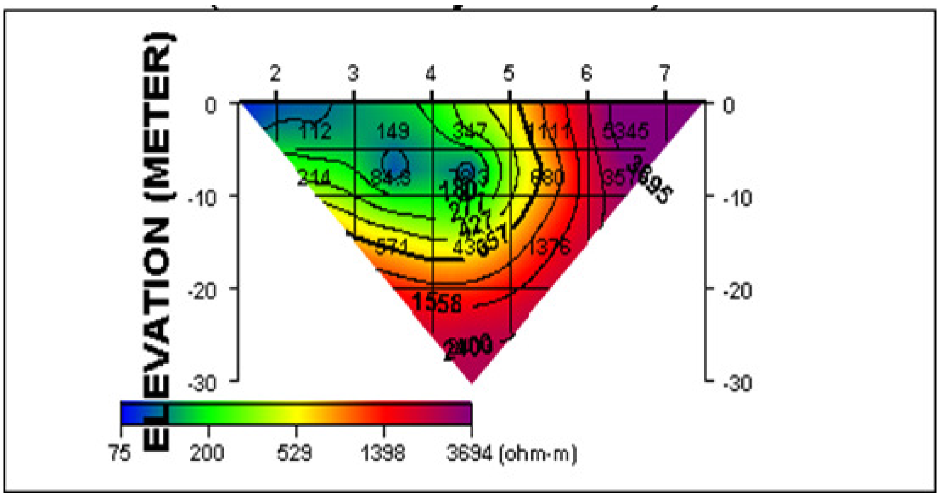

Figure 4 Resistivity Structure along Profile 1

Morrison 1979 or finite-element methods (Silvester and Ferrari 1996). In all optimization methods, an initial model is modified in an iterative manner so that the difference between the model response and the observed data values is reduced.

Apparent resistivity is not the true resistivity because a resistively homogeneous, isotropic subsurface is assumed (Powers et al, 1999). To estimate the true resistivity or the resistivity structure where the subsurface is heterogeneous and/or anisotropic, the apparent resistivity data were processed using DIPPRO inverse modeling software. The inversion results are used to characterize the subsurface resistivity distribution.

RESULTS AND DISCUSSION

The ranges of resistivity values for a single material generally indicate resistivity variations between dry and water-saturated conditions. Dry sands, gravels, and massive unweathered rock typically exhibit relatively high resistivities whereas clays, clayey tills, water-saturated sediments, and weathered rock (chemically broken down to clays) tend to have lower resistivity. However this is not always the case – often wet porous sands will have lower resistivity than tight clay, and a firm understanding of the underlying geology is needed to interpret resistivity cross-sections properly. Shallow geophysics provides the

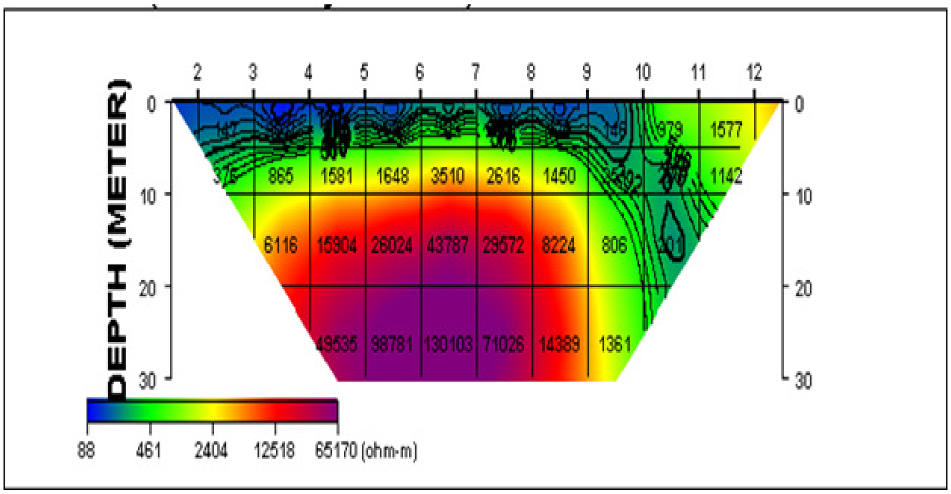

Figure 5 Resistivity Structure along Profile 2

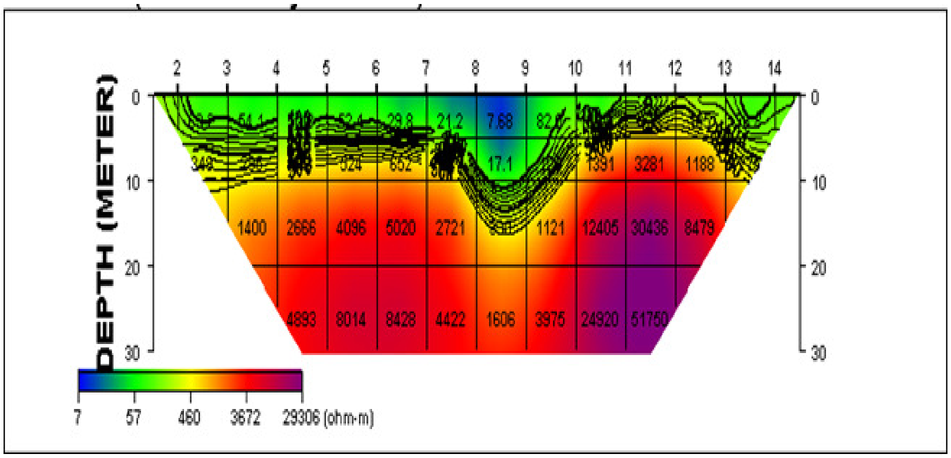

Figure 6 Resistivity Structure along Profile 3

capacity to investigate, detect and map critical subsurface features throughout an area well beyond what can be inferred from borehole drilling programmes alone.

Resistivity data interpretation and presentation comes in different forms. They can be plotted as profile line on a bi-logarithm graph after which they can be matched with master curves for enhance comparison and subsequent interpretation. This process can also be correlated with cumulative plot for layer thicknesses differentiation.

Six traverses with profiles lengths of 70 – 210 m were surveyed in the area. Geoelectric pseudo-sections showing the observed field data, the calculated/theoretical data as well as their corresponding resistivity structures were computed and plotted, however, only the resistivity structures of the traverses are presented, described and discussed in the text.

Profile 1 (Figure 4) covers a distance of 70 m. The resistivity structure shows the basal unit to consist mainly of fresh basement which can be encountered at a depth lower than 15 m below the surface along profile position of 0 – 50 m. The fresh basement outcrops on the surface around the position of 50 – 70 m of the profile length. The fractured part of the basement also outcrops on the surface around 48 - 52 m of the profile length. The fractured basement assumes the curvy structure initiated by the fresh basement structure. Main weathered products consists of gravels (inclined diagonally) with some gravelly sands outcropping on the surface. These sediments occupy the existing curvy structure of the underlying fractures along 0 – 50 m. Thick regolith might have responded favourably to rigorous activities of chemical decomposition of the rocks along weak zones. The actions were mild and/or negligible where fractured and fresh bedrocks outcropped.

Fresh basement rocks of Figure 5 along Profile 2 are observed at the base of the resistivity layer and are located between 30 – 90 m of the profile line. The fresh basement may be traced upwards to depths of 7 m

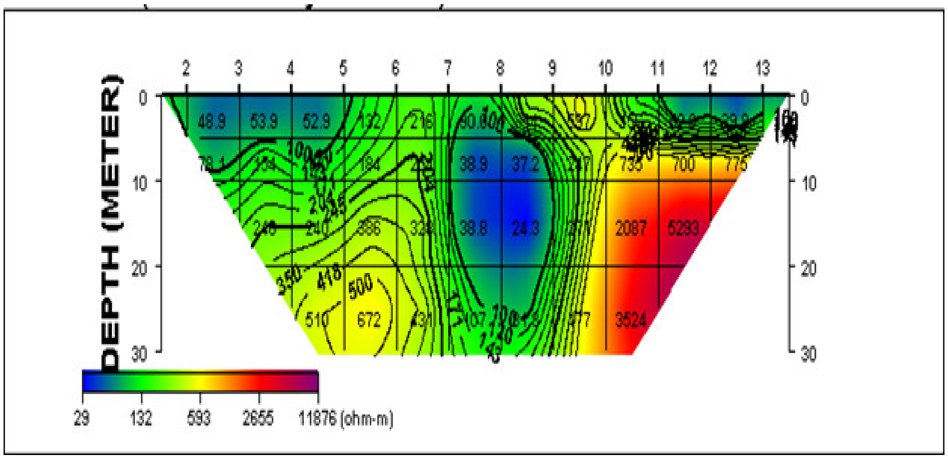

Figure 7 Resistivity Structure along Profile 4

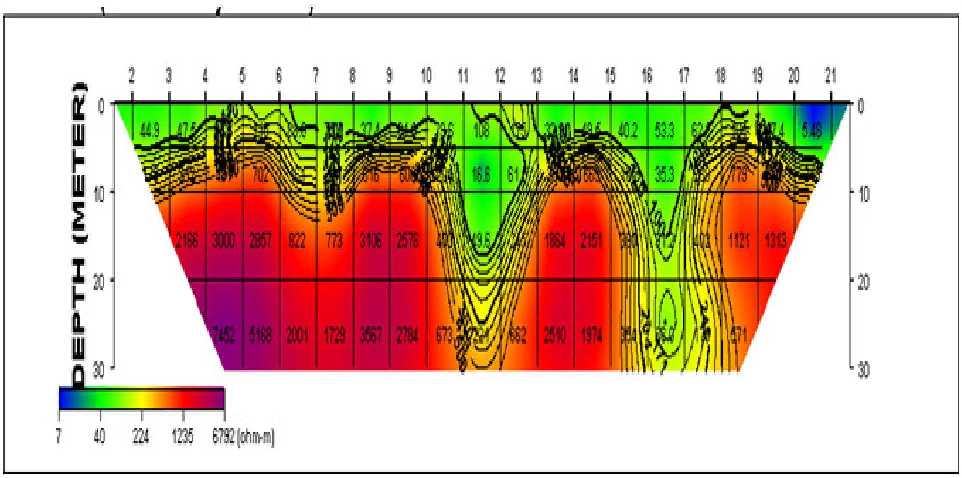

Figure 8 Resistivity Structure along Profile 5

around 60 – 80 m distance and not lower than 15 m below the surface. The section along 90 – 120 m of the profile gives the impression of intensified weathering down to the maximum depth of investigation. The overlying fractured bedrock which dips to the depth of maximum investigation around 90 – 100 m followed the domy structure of the fresh bedrock. Depths at which the fresh basement is buried indicate that weathering was effective, especially along the fractured zone where the fractures and sediments dip to the base of the electrostratigraphy. Few fractures are seen on the surface beyond 117 m distance. Gravel materials exposed on the surface constitute the main capping overburden.

The basal unit of Profile 3 shown by Figure 6 consists of fresh bedrock that is highly affected by fractures along 78 - 95 m distance. Here the fresh rock may be encountered at 15 below the surface. The fresh bedrock occurs as two separate granite bodies probably displaced by faulting where the granite blocks around 100 – 130 m is raised relative to that around 30 – 90 m of the profile length. A fractured zone along 78 - 95 m distance attains a thickness of 10 m. The weathered deposits consist of gravels, sands and clays. Clay matrix which is limited to the highly fractured zone (80 – 90 m) is a minor constituent of the overburden. Stratification of sediments within the fractured zone suggests that suitable grading condition prevailed during deposition.

Figure 7 is a pictorial presentation of the resistivity structure of Profile 4. Fresh bedrock is encountered at a depth of 10 m around 100 – 130 m distance. This suggests that minimum weathered/fractured products may exceed 10 m thick. The effect of fracturing is observed on the surface around 60 – 70 m and 85 – 102 m distances. Resistivity values of the fractures around 35 – 68 m distance of the profile line increase towards the centre of the closure forming a ridge structure. Formation of ridge structure is attributed to the resistance of the rock to weathering. A considerable part of the profile consists of weathered materials from the surface to depth of 30 m.

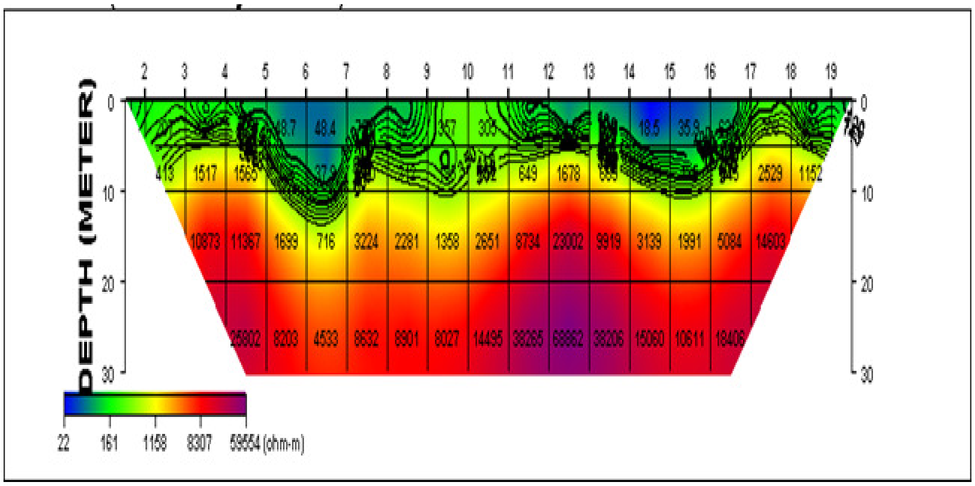

Figure 9 Resistivity Structure along Profile 6

Clayey sands occur in patches around 0 – 50 m, 70 – 90 m and 105 – 130 m. These sediments are enveloped by thin layers of sandy fractions. Thickness of weathered/fractured products suggests that the sediments were not readily removed by later transporting agents. Lens structure of the clays depicts that only a small proportion of its content transported together with the enclosing sediments settled in that environment. Relatively thicker sediments of the profile length suggest that prolong tectonic activity was effective in shattering into pieces and dislodging the pre-existing granites.

Along the area of Profile 5 (Figure 8), fracturing played significant roles on the subsurface structures of the bedrock. Two major and one minor fault are suspected (Sangodigi and Olorunfemi. 2013). The major faults are located along 100 – 130 m and 150 – 180 m distances, and the minor fault is observed along 60 – 80 m of the profile length. Fracturing was intensified within the suspected faulted zones (Alkali, 2013). Some of these fractures appeared on the surface around 48 - 52 m, 112 - 128 m and 180 – 192 m of the profile. The suspected faults seem to have provided pathways for chemical weathering processes that peeled away layers of the rock, giving the fresh bedrocks their characteristic dome tops. Decomposed rock sediments consisting of sandy sequence form the upper lithostratigraphic unit. A small quantity of clay fraction was mapped on the surface to a depth of 4 m at the end of the profile.

Profile 6 (Figure 9) has a resistive basement of fresh granite at its base. The top of the bedrock is wavy and can be traced to a depth not lower than 4 m. Where the bedrock nears the surface, the effect of fracturing is low. Development of deep fractures however, is pronounced along such zones that are weak as demonstrated by electrode positions of 50 – 75 m, 85 – 110 m and 140 – 170 m length of the profile. The fractures are exposed on the surface around 85 -110 m. Weathered regolith consists essentially of gravels, except around zones where the fractures outcropped and around 140 – 150 m zone where sandy gravels were deposited. The undulating structure initiated by the bedrock topography might have conditioned the structures and thicknesses of the overlying formation.

CONCLUSION

Six traverses lengths of between 70 – 210 m were established to survey the subsurface structures in the study area. Tectonic activities played significant roles on the subsurface structures of the bedrock. Fractures on the bedrock tend to provided effective pathways for chemical weathering processes to peel away layers of the rocks, giving the fresh bedrocks characteristic dome tops. Weathering was more effective along such fractured zones where the sediments and fractures dip to the base of the resistivity structure and attain their maximum thicknesses. Resistant rocks tend to form ridge structures in contrast to softer rocks that were easily eroded. Sequence stratigraphy of sediments within the fractured zones suggests suitable grading conditions for the deposits. Lens structures of clays depict that only a small proportion transported with the enclosing sediments settled in the medium. Sinusoidal structures initiated by the bedrock topography tend to control the type of structures formed and thicknesses of the overlying regolith.

REFERENCES

Alkali SC (2013): Mapping and analysis of the density of lineaments around Kagoro Younger granite rocks in North Central Nigeria. Global Advanced Research Journal of Engineering, Technology and Innovation. 2(10): 295 - 303.

Annor AE, Freeth SJ (1985): Thermotectonic evolution of the basement complex around Okene, Nigeria, with special reference to deformation mechanism. Precamb. Res. 28: 269 - 281.

Annor AE, Olasehinde PI, Pal PC (1990): Basement fracture patterns in the control of water channels – an example from Central Nigeria. J. Min. Geol. 26(1): 5 - 12.

Ball E (1980): An example of very consistent brittle deformation over a wide Intra-Continental area. The late Pan African fracture system of the Taureg and Nigerian shield. Tectonophysics. 61: 363 - 379.

Burger HR (1992): Exploration geophysics of the shallow subsurface: Prentice Hall, Inc.

Dey A, Morrison HF (1979): Resistivity modelling for arbitrarily shaped two – dimensional structures. 27(1): 106 –136

Kearey P, Brooks M (1991): An introduction to geophysical exploration. Blackwell scientific publications.

Loke MH (1999): Electrical imaging system for environmental and engineering studies (A practical guide for 2D and 3D surveys). Earth sciences. 6574525. www.terraplus.com.

Loke MH (2004): 2D and 3D Electrical imaging surveys – Tutorial. www.geoelectrical.com.

Olasehinde PI, Pal PC, Annor AE (1990): Aeromagnetic anomalies and structural lineaments in the Nigerian basemen complex. J. Afr. Earth Sci. 11(3, 4): 351-355.

Oyawoye MO (1964): The Geology of the Nigerian basement complex. Journal of Nigeria Mining, Geology and Metallurgical Society, 1(2): 87 – 103.

Powers CJ, Wilson J, Haeni FP, Johnson CD (1999): Surface geophysical characterization of the University of Connecticut Landfill, Storrs, Connecticut: U.S. Geological Survey water-resources investigations Report. 99-4211.

Rahaman MA (1976): Review of the basement geology of South Western Nigeria. In: Kogbe CA (ed). Geology of Nigeria. Elizabethan publishing company, Lagos. 41 - 58.

Rahaman MA (1988): Recent advances in the study of the basement complex of Nigeria. In: Precambrian geology of Nigeria. Geological Survey of Nigeria publication, Kaduna. 11- 43.

Sangodigi EE, Olorunfemi MO (2013): Geophysical investigation of a suspected foundation failure at Ogbomoso, Southwestern Nigeria. Pacific Journal of Science and Technology. 14(2): 522 - 536.

Silvester PP, Ferrari RL (1996): Finite elements for electrical engineers. Cambridge University press.

Telford WM, Geldart LP, Sheriff RE, Keys DA (1976): Applied geophysics. Cambridge University press.

Wright JB, McCurry P (1970): The geology of Nigeria sheet 102 SW, Zaria and its regions. Mortimore, M. J.(ed). Department of Geography, Occasional paper. Ahmadu Bello University, Zaria. 4.